Received: 19 March 2021 | Accepted: 22 April 2021

DOI: 10.1111/1759-7714.13993

ORIGINAL ARTICLE

WILEY

Circular RNA circLDB2 functions as a competing endogenous RNA to suppress development and promote cisplatin sensitivity in non-squamous non-small cell lung cancer

Yuanyuan Wang[1] | Luguang Li[2] | Weiyu Zhang[2] | Guojun Zhang[1]

[1]Department of Pulmonary and Critical Care Medicine, The First Affiliated Hospital of Zhengzhou University, Zhengzhou, China

[2]Department of Pulmonary and Critical Care Medicine, The First Affiliated Hospital of Henan University of Chinese Medicine, Zhengzhou, China

Correspondence
Guojun Zhang, Department of Pulmonary and Critical Care Medicine, the First Affiliated Hospital of Zhengzhou University, No. 1 Jianshe East Road, Zhengzhou 450052, China.
Email: zgj@zzu.edu.cn

Abstract

Background: Circular RNAs (circRNAs) are covalently closed RNAs and are implicated in the development of non-small cell lung cancer (NSCLC). Here, we identified the precise actions of circRNA LIM domain binding 2 (circLDB2, hsa_circ_0069244) in non-squamous NSCLC development and drug sensitivity.

Methods: CircLDB2, microRNA (miR)-346, and LIM and calponin-homology domains 1 (LIMCH1) were quantified by quantitative real-time polymerase chain reaction (qRT-PCR) or western blot. Ribonuclease R (RNase R), actinomycin D, and subcellular localization assays were used to characterize circLDB2. Cell proliferation and viability, colony formation, apoptosis, migration, and invasion were gauged by Cell Counting Kit-8 (CCK-8), colony formation, flow cytometry, wound-healing, and transwell assays, respectively. RNA immunoprecipitation (RIP), RNA pull-down, and dual-luciferase reporter assays were used to verify the direct relationship between miR-346 and circLDB2 or LIMCH1. Animal studies were performed to evaluate the impact of circLDB2 in vivo.

Results: CircLDB2 was underexpressed in non-squamous NSCLC and was identified as a bona fide circular transcript. Overexpression of circLDB2 impeded cell proliferation, migration, invasion, and enhanced apoptosis and cisplatin sensitivity in vitro, as well as promoted the antitumor effect of cisplatin in vivo. CircLDB2 regulated cell functional behaviors and cisplatin sensitivity by sponging miR-346. LIMCH1 was a direct and functional target of miR-346. Furthermore, circLDB2 acted as a competing endogenous RNA (ceRNA) for miR-346 to induce LIMCH1 expression.

Conclusion: Our findings demonstrated that circLDB2 impeded non-squamous NSCLC development and enhanced cisplatin sensitivity partially by acting as a ceRNA, highlighting circLDB2 as a promising candidate for the development of novel antitumor therapies.

KEYWORDS
circLDB2, LIMCH1, miR-346, non-squamous NSCLC

INTRODUCTION

Despite decades of research, non-small cell lung cancer (NSCLC), including non-squamous NSCLC, remains the leading cause of cancer mortality globally.[1] Although surgery, chemotherapy, and radiotherapy can effectively control primary tumors, these therapies have limits in curbing metastatic non-squamous NSCLC.[2] Cisplatin-based chemotherapy has been widely used for treatment of non-squamous NSCLC,[3,4] however, drug resistance frequently arises.[5] Investigation of the alterations of important regulatory molecules, including circular RNAs (circRNAs) and proteins that drive NSCLC is ongoing.[6,7] Understanding the actions of these molecules will provide a novel opportunity

for developing molecularly targeted therapies for non-squamous NSCLC.

CircRNAs are covalently closed RNAs, and numerous circRNAs are generated by head-to-tail splicing of exons of messenger RNAs (mRNAs).[8] Many circRNAs can form a novel type of post-transcriptional regulators by operating as competing endogenous RNAs (ceRNAs).[9] Recent studies have documented the ceRNA function of some circRNAs by sequestering microRNAs (miRNAs) in modulating the development of human cancers, including NSCLC.[10,11] For example, Chen et al.[12] illuminated that circ_100 146 functioned a ceRNA for miR-615-5p and miR-361-3p to promote NSCLC development via inducing splicing factor 3b subunit 3 expression. Xu et al.[13] demonstrated the regulation of circ_0014235/miR-520a-5p/cyclin-dependent kinase 4 (CDK4) ceRNA network in NSCLC development and cisplatin resistance. However, the critical, precise actions of circRNAs in the development of non-squamous NSCLC largely remain to be elucidated.

MiRNAs are attractive candidates as upstream modulators of human tumorigenesis, and aberrant miRNA expression has been shown in various cancers including NSCLC.[14,15] Previous work demonstrated miR-346, an overexpressed miRNA in NSCLC, with the ability to accelerate NSCLC cell malignant behaviors.[16] Nevertheless, it is still undefined whether miR-346 can work as a functional mediator of circRNAs in non-squamous NSCLC development and drug sensitivity.

In a preliminary survey, when we used the online dataset (GSE112214, https://www.ncbi.nlm.nih.gov/geo/geo2r/?acc=GSE112214) to analyze the differentially expressed circRNAs in NSCLC development we found that circRNA LIM domain binding 2 (circLDB2, hsa_circ_0069244) was the greatest differentially expressed circRNA. Moreover, no reports showed whether circLDB2 expression is causally involved in the development of non-squamous NSCLC. Here, we undertook to explore the precise roles of circLDB2 in the functional behaviors and cisplatin sensitivity of non-squamous NSCLC cells. We also identified a novel endogenous competition among circLDB2, miR-346, LIM, and calponin-homology domains 1 (LIMCH1), a well-known tumor inhibitor in NSCLC.[17,18]

MATERIALS AND METHODS

Bioinformatics

To search the differentially expressed circRNAs in NSCLC, we used an online dataset (GSE112214) of the Gene Expression Omnibus (GEO) database ($p < 0.05$, $|\log_2 FC| > 1$) (https://www.ncbi.nlm.nih.gov/geo/geo2r/?acc=GSE112214). To analyze the abnormally expressed genes in non-squamous NSCLC, we used the online dataset (GSE108214) of the GEO database (https://www.ncbi.nlm.nih.gov/geo/query/acc.cgi?acc=GSE108214) and GEPIA database (http://gepia.cancer-pku.cn/detail.php). To visualize circLDB2, we used online software CircView (http://gb.whu.edu.cn/CircView/). The binding sites of miRNAs to circLDB2 were predicted by two computer algorithms circinteractome (https://circinteractome.nia.nih.gov/) and starBase (http://starbase.sysu.edu.cn/). The molecular targets of miR-346 were predicted by starBase software.

Human clinical samples and cell lines

Primary lung tumors and adjacent normal lung tissues were harvested and processed in compliance with a protocol approved by the Ethics Committee of the First Affiliated Hospital of Henan University of Chinese Medicine. Fresh tissues were obtained from non-squamous NSCLC patients at the First Affiliated Hospital of Henan University of Chinese Medicine, paraffin-embedded or snap-frozen, and preserved at −80°C. All patients gave written informed consent. Immunohistochemistry for LIMCH1 expression analysis was carried out on the paraffin-embedded tissues according to the standard method as reported,[19] using LIMCH1 antibody (1:500, ab96178, Abcam). Frozen tissues were used to quantify the expression of circLDB2, miR-346 and LIMCH1 by using quantitative real-time polymerase chain reaction (qRT-PCR) or western blot as below.

A549, H23, and H460 non-squamous NSCLC cells were obtained from American Type Culture Collection (ATCC) and the normal bronchial 16HBE cell line because the control was from Procell. All cell lines were propagated with 10% fetal calf serum and 1% antibiotics in RPMI-1640 medium (all from Sigma-Aldrich) in 5% CO_2 at 37°C.

Generation of stable circLDB2 overexpressing cell line

Human circLDB2 (hsa_circ_0069244) sequence and the scrambled control sequence were synthesized by GeneCreate and directionally cloned in the EcoR I and BamH I sites of pLC5-ciR lentiviral vector (Geneseed). Lentivirus was produced by cotransfection of the above constructs with psPAX2 and pMD2.G packaging plasmids (Addgene) into the HEK293T cells (ATCC). A549 and H460 cells were transduced by the lentiviral particles (circLDB2 and vector) using 5 μg/mL polybrene (Yesen). Transduced cells were selected in 2 μg/mL puromycin (Sigma-Aldrich) to generate stable cell lines.

Transient transfection of cells

Cultured A549 and H460 cells in 24-well plates at 5×10^4 per well were transiently transfected with synthetic miR-346 mimic (50 nM) or a negative control oligonucleotide (miR-NC, 50 nM), miR-346 inhibitor (anti-miR-346, 60 nM) or a negative control inhibitor (anti-NC, 60 nM), and LIMCH1-shRNA vector (sh-LIMCH1) or non-target

shRNA (sh-NC) at a final dose of 200 ng using Lipofectamine 3000 per manufacturer's recommendations (Thermo Fisher Scientific). All shRNA constructs and oligonucleotides were from Ribobio and described in Table S1. Experiments were carried out 48 hours after transfection.

RNA isolation and qRT-PCR

For RNA extraction from cells and tissues, the mirVana miRNA Isolation Kit was used as recommended by the manufacturers (Thermo Fisher Scientific). For circLDB2 and mRNA analysis, cDNA was randomly primed or synthesized with oligo(dT)18 primers from 1 μg of RNA using the Omniscript RT Kit (Qiagen), and diluted cDNA was used for qRT-PCR with SYBR Green (TaKaRa) on an iCycler (Bio-Rad). β-actin served as a normalization control. For miR-346 analysis, qRT-PCR was done as above with TaqMan miRNA assay as per the manufacturing protocols (Applied Biosystems). Amplification of U6 was used for normalization. All qRT-PCR primers were from GeneCreate and described in Table S1.

Ribonuclease R, actinomycin D, and subcellular localization assays

In ribonuclease R (RNase R) experiments, 5 μg RNA of H460 or A549 cells was incubated with RNase R (Geneseed) for 20 minutes at 37°C. In subcellular localization experiments, cytoplasmic and nuclear RNA of H460 and A549 cells were individually isolated using the Cytoplasmic and Nuclear RNA Purification Kit as described by the manufacturers (Norgen Biotek). For actinomycin D treatment, A549 and H460 cells were plated in 24-well cell culture dishes at 1×10^4 per well in complete medium containing 5 μg/mL of actinomycin D (Sigma-Aldrich) for the indicated time point.

Cell proliferation, survival, colony formation, and apoptosis assays

H460 and A549 cells were performed various transductions or transfections as above. Cell proliferation was monitored every 24 hours using the Cell Counting Kit-8 (CCK-8) assay as per the manufacturing guidance (Beyotime). For the assessment of the half maximal inhibitory concentration (IC50) for cisplatin, cultured cells were exposed to the indicated concentration of cisplatin (Sigma-Aldrich) for 48 hours, and IC_{50} value was calculated following curve fitting to the cell survival data after the accomplishment of CCK-8 assay. Cell colony formation was measured using a standard method as reported,[20] and five random fields of each sample were manually counted. Cell apoptosis was gauged using the annexin V-fluorescein isothiocyanate (FITC)/propidium iodide Apoptosis Detection Kit (Beyotime) and then analyzed on a FACScan (BD Biosciences) with FlowJo software (Tree Star).

Cell migration and invasion assays

For migration analysis, a wound-healing assay was carried out as reported.[21] Briefly, a vertical scratch was created with a sterile pipette tip (200 μL) on a confluent cell monolayer. Wound healing was analyzed after 24 hours culture using ImageJ software (National Institutes of Health) accompanying the inverted 10 × microscope (Carl Zeiss). For invasion assay, 1×10^5 indicated cells cultured in serum-free medium were plated in a Matrigel-coated chamber with 8 μm pores (BD Biosciences) and allowed to invade toward a 15% serum gradient for 24 hours. Cells that remained on the top of the insert were scrubbed off, and cells that traversed the membranes were stained with 0.2% crystal violet (Yesen). Ten random fields of each sample were counted under the 100× microscope with ImageJ software.

Western blot

Lysates were obtained by lysing cells and tissues (0°C, 30 minutes) in RIPA buffer (Yesen) containing proteinase and phosphatase inhibitors (Sigma-Aldrich), resolved by electrophoresis, and transferred to a polyvinylidene fluoride membrane (BD Biosciences). Blots were probed with primary antibodies against p53 (anti-p53, 1:500, MA5-14516), B-cell lymphoma 2 binding component 3 (anti-PUMA, 1:1000, PA5-20007), LIMCH1 (anti-LIMCH1, 1:2000, PA5-34745), loading control β-actin (anti-β-actin, 1:1500, PA1-183), and horseradish peroxidase-linked IgG secondary antibody (1:10,000, G-21234, all from Invitrogen). The ImageGauge Program (Fuji Film) was used for densitometric analysis of protein blots.

RNA immunoprecipitation and RNA pull-down assays

Lysates were prepared by lysing A549 and H460 cells (0°C, 30 minutes) using RNA immunoprecipitation (RIPA) buffer. For RIP experiments, lysates were incubated with antibody against Argonaute 2 (anti-Ago2, 1:500, MA5-23515) or isotype IgG (anti-IgG, 1:1000, 05–4500, all from Invitrogen) and Protein A/G Magnetic Beads (Thermo Fisher Scientific) overnight at 4°C. For RNA pull-down experiments, lysates were incubated with biotinylated circLDB2 probe (WT-circLDB2 probe), biotinylated circLDB2 mutant probe in the target region (MUT-circLDB2 probe), or negative control oligo probe (all from Ribobio) and streptavidin beads (Invitrogen) overnight at 4°C. In both experiments, bound RNA was harvested from beads and used for the assessment of circLDB2 and miR-346 levels.

Dual-luciferase reporter assay

The segments of circLDB2 (hsa_circ_0069244) and LIMCH1 3'UTR were synthesized by GeneCreate and individually cloned in the Spel and Mlul sites of the pMIR-REPORT luciferase vector (Thermo Fisher Scientific), and the GGCAGAC seed sequence was mutated to CCGUCUG using the TaKaRa MutanBest Kit (TaKaRa). Each reporter plasmid (200 ng) and pRL-TK vector (50 ng for normalization, Promega) was cotransfected with Lipofectamine 3000 into A549 and H460 cells in 24-well cell culture dishes (5×10^4 per well), together with either miR-346 mimic or mimic control at 50 nM. Cells were harvested after 48 hours for assay using the Dual-luciferase reporter assay system as recommended by the manufacturers (Promega).

Animal studies

Experiments on mice were carried out in accordance with the protocols approved by the Animal Care Committee of the First Affiliated Hospital of Henan University of Traditional Chinese Medicine. Fifteen 4- to 5-week-old BALB/c nude mice (Jiangsu ALF Biotechnology) were randomly assigned to three groups ($n = 5$ per group): vector, cisplatin + vector, and cisplatin + circLDB2. For the xenograft tumor generation, 2×10^6 vector-infected ($n = 10$ mice) or circLDB2-transduced ($n = 5$ mice) A549 cells were injected subcutaneously into the flanks of the nude mice. For cisplatin treatment, when these tumors reached an approximate average volume of 100 mm^3, these mice were injected intraperitoneally by cisplatin (2 mg/kg) or the same amount of saline twice a week. The volume of the tumor was periodically calculated using the equation length $\times$ width^2 $\times$ 0.5. Tumors were harvested from the sacrificial mice at day 28 after cell implantation.

Statistical analysis

All experiments were performed at least three independent biological replicates. Data were presented as mean $\pm$ standard deviation. Statistical analysis was done by the SPSS 18.0 software (SPSS). A Student's *t*-test, Mann–Whitney *U* test, and analysis of variance (ANOVA) with LSD or Dunnett's post hoc test were used according to the type of experiment, with $p < 0.05$ considered significant.

RESULTS

CircLDB2 was underexpressed in non-squamous NSCLC

To search for circRNAs potentially involved in NSCLC development, we used the online dataset (GSE112214) of GEO database. Volcano plot showed many differentially expressed circRNAs in NSCLC tissues compared with normal controls, and circLDB2 was the greatest differentially expressed circRNA (Figure 1(a)). The dataset data also revealed the remarkable downregulation of circLDB2 in NSCLC samples (Figure 1(b)). We analyzed circLDB2 expression in 53 primary tumors and adjacent noncancerous lung tissues from the same patients with non-squamous NSCLC. As demonstrated by qRT-PCR, circLDB2 was markedly underexpressed in non-squamous NSCLC samples compared with normal controls (Figure 1(c)). Moreover, circLDB2 expression was associated with tumor, node, and metastasis (TNM) stage and lymph node metastasis of these tumors (Figure 1(d),(e)). In agreement with tumor samples, non-squamous NSCLC cells (A549, H23, and H460) exhibited lower levels of circLDB2 compared with normal 16HBE cells (Figure 1(f)). Together, these results indicated the downregulation of circLDB2 in non-squamous NSCLC.

Identification of circLDB2

As shown in Figure 2(a), circLDB2 was a 483-nucleotide long circRNA that was produced by the back-splicing of exons 2, 3, 4, and 5 of LDB2 mRNA. The back splicing junction was confirmed by Sanger sequencing (Figure 2(a)). To address the closed loop structure of circLDB2, we used random and oligo(dT)18 primers for reverse transcription before qRT-PCR analysis. Owing to the depletion of poly(A) tails on circRNAs, the circLDB2 level was lower in the oligo(dT)18 primer group than that in the random primer group (Figure 2(b) and (c)). Using cDNA and genomic DNA (gDNA) of A549 and H460 cells as templates, circLDB2 was amplified by the divergent primers on cDNA rather than gDNA (Figure 2(d)). We performed RNase R and actinomycin D assays to evaluate the stability of circLDB2. RNase R results showed that circLDB2, rather than the corresponding linear LDB2 mRNA (mLDB2), was resistant to RNase R (Figure 2(e),(f)). The incubation of cells with actinomycin D caused a significant reduction in mLDB2 level, and circLDB2 expression was not reduced in the assayed time frame (Figure 2(g),(h)). Furthermore, subcellular localization assays showed that circLDB2 was mainly present in the cytoplasm of A549 and H460 cells (Figure 2(i), (j)). All these results indicated that circLDB2 was a bona fide circular transcript.

Overexpression of circLDB2 repressed cell proliferation, migration, invasion, and promoted apoptosis and cisplatin sensitivity in vitro

To evaluate the functional role of circLDB2 in non-squamous NSCLC development and chemosensitivity, we overexpressed circLDB2 using an overexpression lentivirus

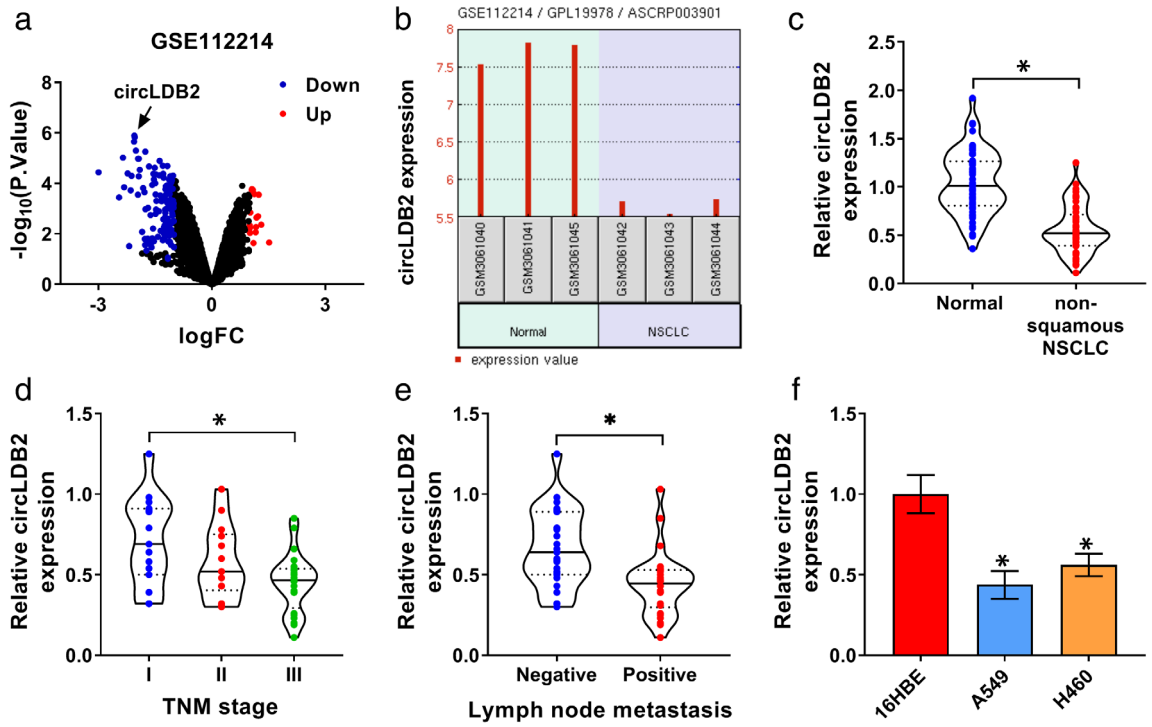

FIGURE 1 CircLDB2 expression was decreased in non-squamous NSCLC. (a) Volcano plot shows the differentially expressed circRNAs in three pairs of NSCLC samples and adjacent normal tissues using the GEO database (GSE112214). (b) GEO database (GSE112214) showing the underexpression of circLDB2 in three pairs of NSCLC samples and adjacent normal controls. (c) qRT-PCR analysis of circLDB2 in 53 primary tumors and adjacent noncancerous lung tissues from the same patients with non-squamous NSCLC. (d) CircLDB2 expression by qRT-PCR analysis in tumor samples distributed in TNM stage I ($n = 15$), II ($n = 14$) and III ($n = 24$). (e) qRT-PCR analysis showing the expression of circLDB2 in negative-lymph node metastasis tumors ($n = 27$) and positive-lymph node metastasis tumors ($n = 26$). (f) qRT-PCR analysis showing the underexpression of circLDB2 in A549, H23, and H460 non-squamous NSCLC cells compared with 16HBE cells. *$p < 0.05$

system in A549 and H460 cells (Figure 2(k),(l)). Remarkably, circLDB2 overexpression suppressed cell proliferation (Figure 3(a),(b)), colony formation (Figure 3(c)), and enhanced cell apoptosis (Figure 3(d)), as well as impeded cell migration (Figure 3(e)) and invasion (Figure 3(f)). Moreover, elevated expression of circLDB2 reduced the IC50 for cisplatin in the two cell lines, indicating that circLDB2 overexpression enhanced cisplatin sensitivity (Figure 3(g),(h)). Additionally, A549 and H460 cells stably expressing circLDB2 exhibited increased levels of tumor suppressor protein p53 and pro-apoptotic protein PUMA compared with negative controls (Figure 3(i),(j)). Taken together, these results demonstrated that circLDB2 overexpression modulated cell functional behaviors and cisplatin sensitivity in vitro.

CircLDB2 regulated cell functional behaviors and cisplatin sensitivity in vitro by sequestering miR-346

To elucidate the molecular basis underlying the regulation of circLDB2 in non-squamous NSCLC development and chemosensitivity, we used computer algorithms to identify the targeted miRNAs of circLDB2. Intriguingly, a putative miR-346 binding region within circLDB2 was predicted by both starBase and circinteractome search programs (Figure 4(a)). Analysis of miR-346 expression in tumor samples and cells showed that miR-346 was markedly overexpressed in non-squamous NSCLC tissues and cell lines compared with their counterparts (Figure 4(b) and (c)). MiRNAs silence target mRNAs in the cytoplasm in the form of miRNA ribonucleoprotein complex (miRNP) that also contains Ago2, the core component of the RNA-induced silencing complex (RISC).[22] Therefore, we performed RIP experiments using anti-Ago2 antibody. The incubation of cell lysates with anti-Ago2 antibody led to a significant increase in the enrichment levels of circLDB2 and miR-346 (Figure 4(d),(e)), indicating that circLDB2 could present in the RISC. Computer algorithms predicted that there were seven binding sites for miR-346 within circLDB2 (Figure 4(f)). To validate the validity of the binding sites, we adopted dual-luciferase reporter assays. Notably, overexpression of miR-346 by miR-346 mimic transfection (Figure 4(g)) repressed the luciferase activity of circLDB2 reporter construct (Figure 4(h),(i)). Mutation of the putative miR-346 binding sites (Figure 4(f)) in the reporter vector abolished the suppression of miR-346 (Figure 4(h),(i)). Furthermore, RNA pull-down assays demonstrated that biotinylated

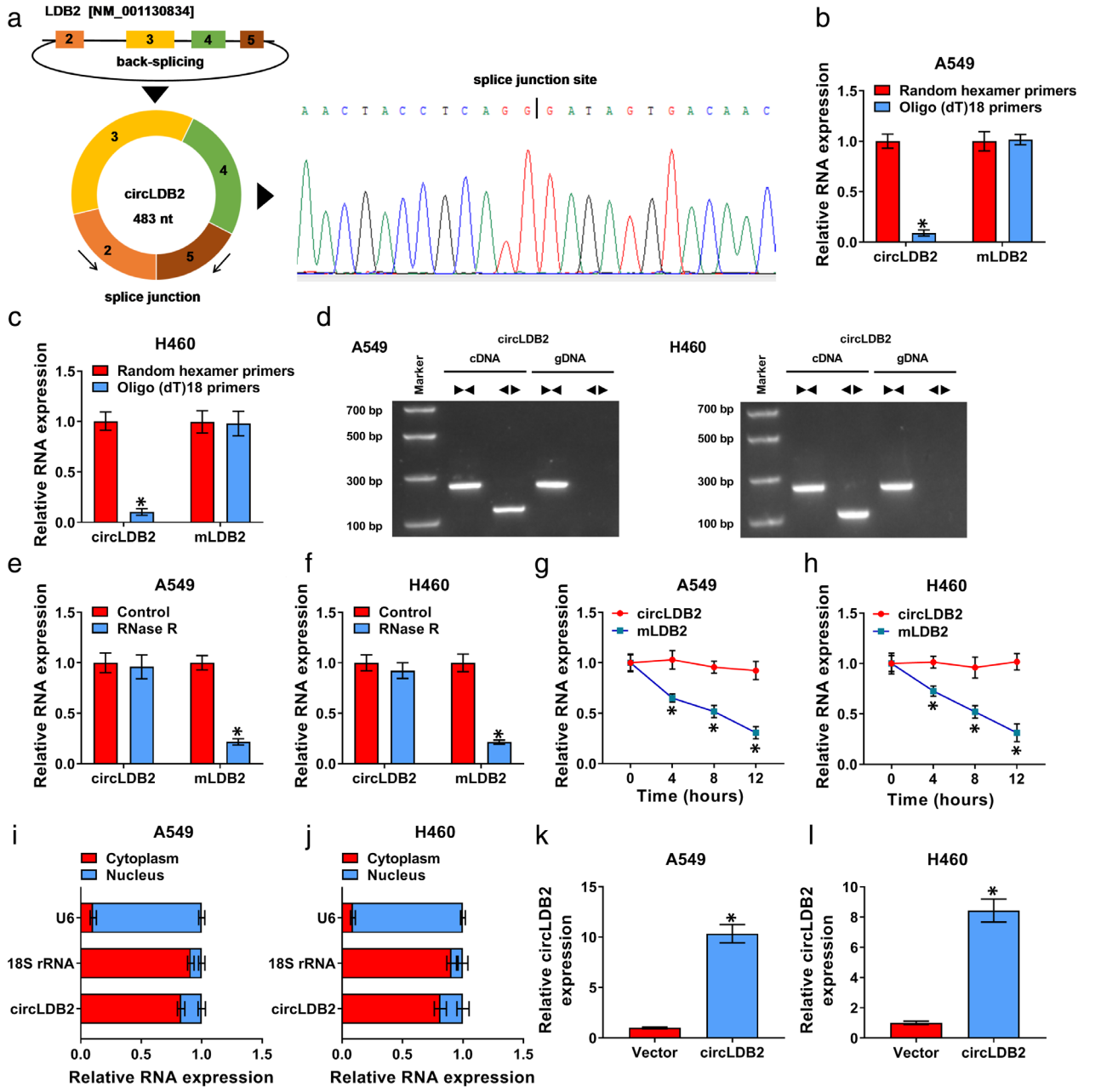

FIGURE 2 CircLDB2 was a bona fide circular transcript. (a) Schematic diagram of circLDB2 circularization by the back-splicing of exons 2, 3, 4, and 5 of LDB mRNAs, and the back-splice junction site identified by sanger sequencing. (b) and (c) the levels of circLDB2 and corresponding linear LDB2 mRNA (mLDB2) by qRT-PCR analysis before using random hexamer and oligo(dT)18 primers for reverse transcription. (d) Amplification of circLDB2 using divergent and convergent primers with cDNA and gDNA as templates and representative pictures of agarose electrophoresis. (e) and (f) RNase R assays in both A549 and H460 cell lines. (g) and (h) actinomycin D assays in A549 and H460 cells. (i) and (j) subcellular localization assays in A549 and H460 cells. (k) and (l) qRT-PCR analysis of circLDB2 expression in cells transduced with negative control lentivirus (vector) or circLDB2 overexpression lentivirus (circLDB2). *$p < 0.05$

circLDB2 probe (WT-circLDB2 probe) remarkably increased the enrichment level of miR-346, and this effect was abolished by biotinylated circLDB2 mutant probe in the target region (MUT-circLDB2 probe) (Figure 4(j),(k)), indicating that miR-346 could bind to circLDB2 by the predicted miR-346 target binding sites. All these results indicated that circLDB2 harbored effective binding sites for miR-346.

Next, we determined whether circLDB2 modulated non-squamous NSCLC development and chemosensitivity by operating as a sponge of miR-346. As expected, the transfection of miR-346 mimic markedly abolished circLDB2 overexpression-mediated anti-proliferation (Figure 5(a),(b)), anti-colony formation (Figure 5(c)), pro-apoptosis (Figure 5(d)), anti-migration (Figure 5(e)), and anti-invasion (Figure 5(f)) effects. Moreover, overexpression of miR-346

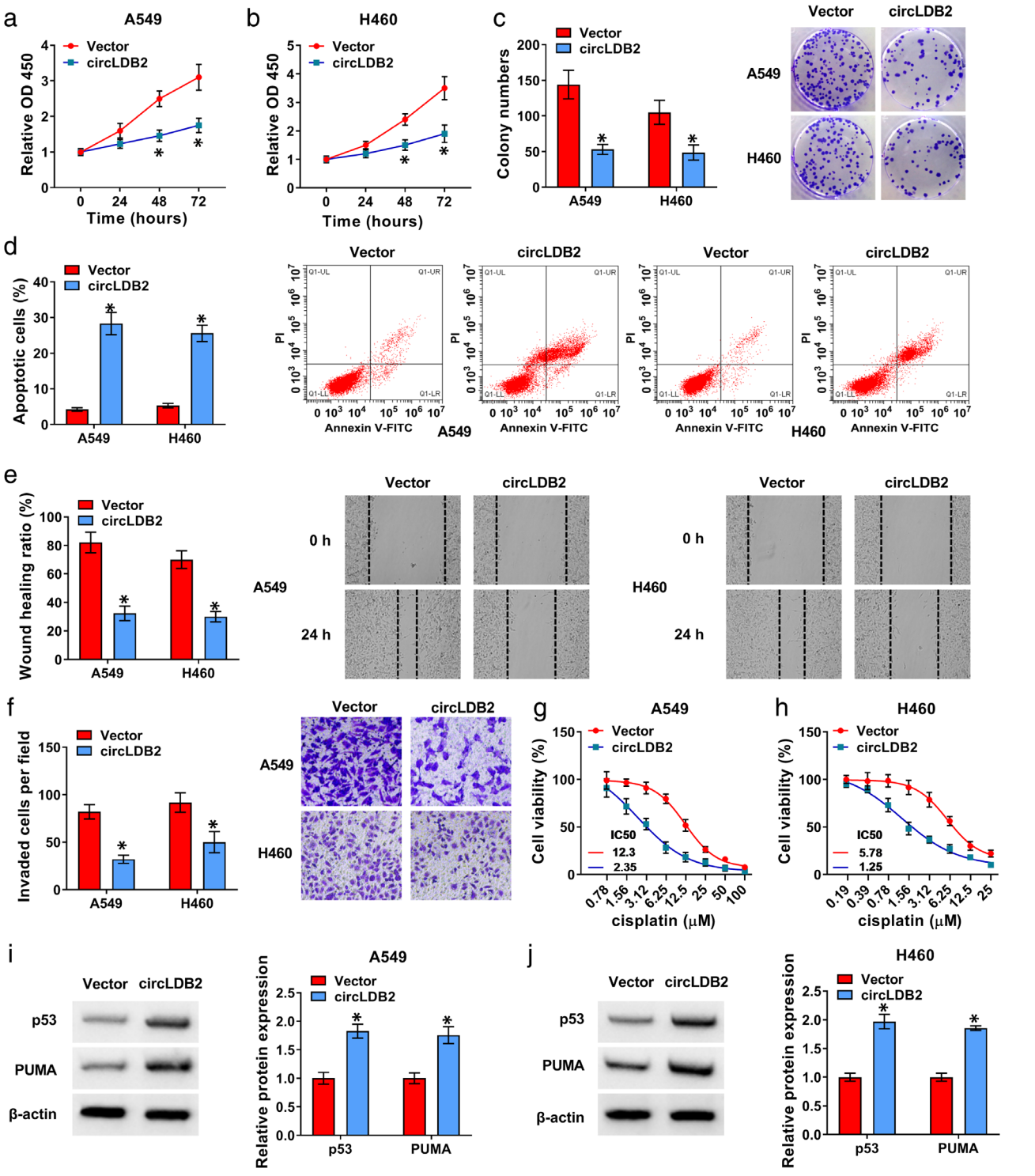

FIGURE 3 CircLDB2 overexpression regulated cell proliferation, apoptosis, migration, invasion, and cisplatin sensitivity in vitro. A549 and H460 cells were transduced with negative control lentivirus (vector) or circLDB2 overexpression lentivirus (circLDB2). (a) and (b) CCK-8 assay of proliferation of transduced cells. (c) Representative images depicting a colony formation assay and colony formation assay of colony formation ability. (d) Representative images depicting a cell apoptosis assay and cell apoptosis by flow cytometry. (e) Representative images showing a cell migration assay and cell migration by wound-healing assay. (f) Representative images showing a cell invasion assay and cell invasion by transwell assay. (g) and (h) CCK-8 assay of viability of transduced cells under cisplatin (various doses) exposure. (i) and (j) representative images depicting a western blot assay and western blot showing the levels of p53 and PUMA in transduced cells. $^*p < 0.05$

significantly counteracted circLDB2 overexpression-mediated reduction of the IC50 for cisplatin (Figure 5(g),(h)) and enhancement of p53 and PUMA levels (Figure 5(i),(j)). Together, these results strongly established the notion that circLDB2 regulated non-squamous NSCLC development and cisplatin sensitivity in vitro through sequestering miR-346.

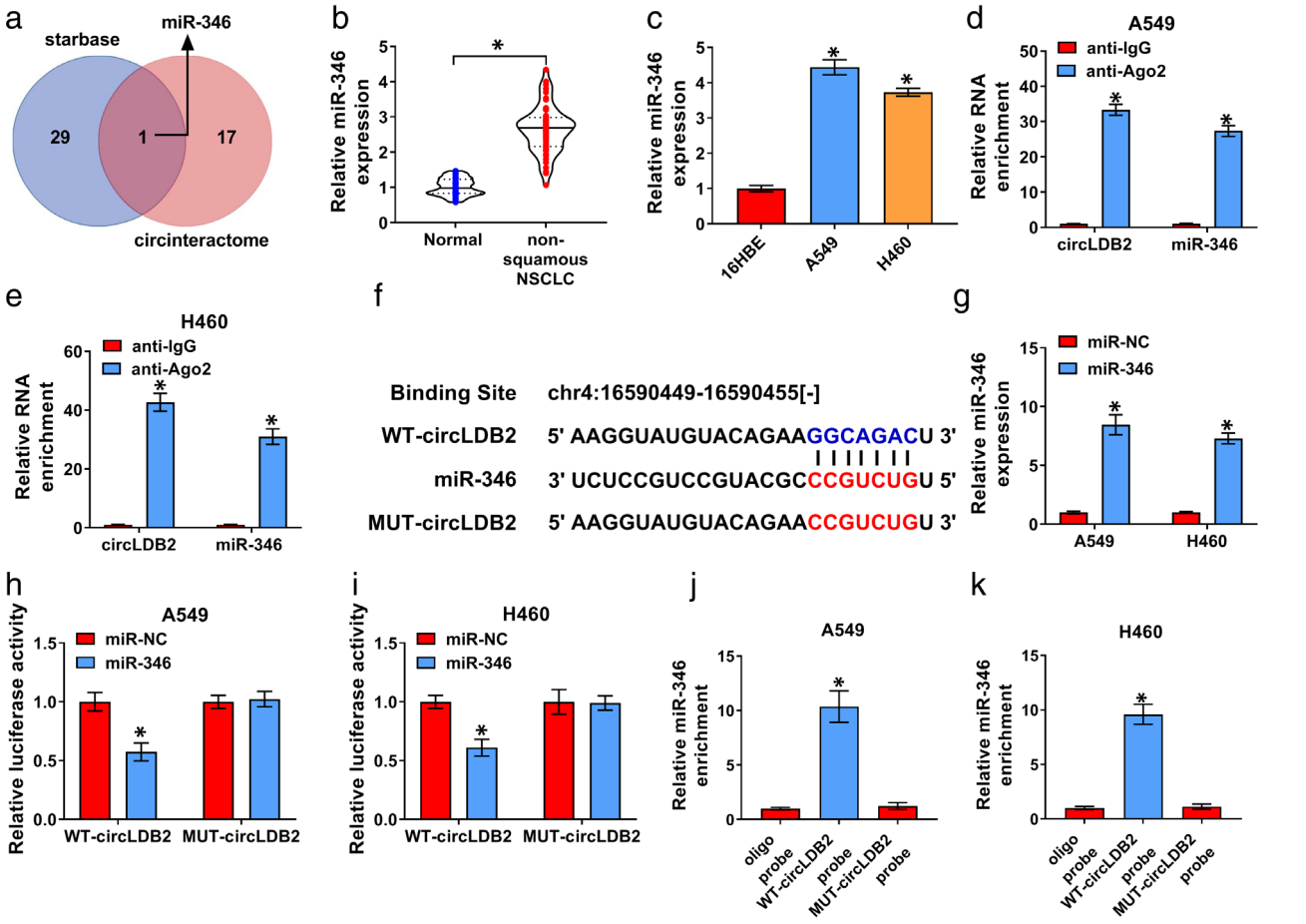

FIGURE 4 CircLDB2 harbored effective binding sites for miR-346. (a) Venn diagram showing the putative targeted miRNAs of circLDB2 predicted by both starBase and circinteractome search programs. (b) qRT-PCR analysis of miR-346 in 53 primary tumors and adjacent noncancerous lung tissues from the same patients. (c) qRT-PCR analysis revealing miR-346 expression in 16HBE, A549, and H460 cells. (d) and (e) RIP experiments in A549 and H460 cells using anti-Ago2 or anti-IgG antibody. (f) Sequence of miR-346, the miR-346 binding sites within circLDB2 and the mutant of the target region. (g) qRT-PCR analysis of miR-346 in cells transfected with miR-346 mimic or miR-NC mimic. (h) and (i) dual-luciferase reporter assays in A549 and H460 cells with circLDB2 wild-type (WT-circLDB2) or mutant (MUT-circLDB2) luciferase reporter constructs. (j) and (k) RNA pull-down assays in A549 and H460 cells using biotinylated circLDB2 probe (WT-circLDB2 probe), biotinylated circLDB2 mutant probe in the target region (MUT-circLDB2 probe), or negative control oligo probe. *$p < 0.05$

CircLDB2 acted as a ceRNA for miR-346 to induce LIMCH1 expression

To identify downstream targets of miR-346, we used mRNA target-prediction program starBase based on the presence of binding sites in the 3'UTR. By combining starBase predicted results and the 100 most significantly underexpressed genes in cisplatin-resistant A549 cells from the online dataset (GSE108214) of the GEO database, we found five targets including LIMCH1, CUB domain-containing protein 1 (CDCP1), docking protein 7 (DOK7), EPS8 like 1 (EPS8L1), and mesothelin (MSLN) (Figure 6 (a)). Interestingly, among these targets, LIMCH1 was the only significantly downregulated gene in lung adenocarcinoma (LUAD) tissues compared with the controls analyzed by the GEPIA database (Figure 6(b) and Figure S1). The data of qRT-PCR analysis validated the downregulation of LIMCH1 mRNA in non-squamous NSCLC samples (Figure 6(c)). In line with qRT-PCR analysis, immunohistochemistry assays showed low LIMCH1 expression in non-squamous NSCLC samples compared with normal controls (Figure 6(d)). Moreover, non-squamous NSCLC tissues and cells exhibited lower levels of LIMCH1 protein and mRNA, respectively, compared with their counterparts (Figure 6(e) and (f)). Interestingly, the target-prediction program starBase showed a putative miR-346 binding sequence in the 3'UTR of LIMCH1 mRNA (Figure 6(g)). To confirm this, we generated 3'UTR wild-type or mutant-type luciferase reporter constructs and analyzed them by luciferase activity. Cotransfection of the luciferase reporter plasmid and miR-346 mimic into the two cell lines produced lower luciferase activity than cells cotransfected with miR-NC mimic but mutation of the target region markedly abrogated the repression of miR-346 (Figure 6(h) and (i)). We tested whether miR-346 could influence LIMCH1 expression. The transfection efficiency

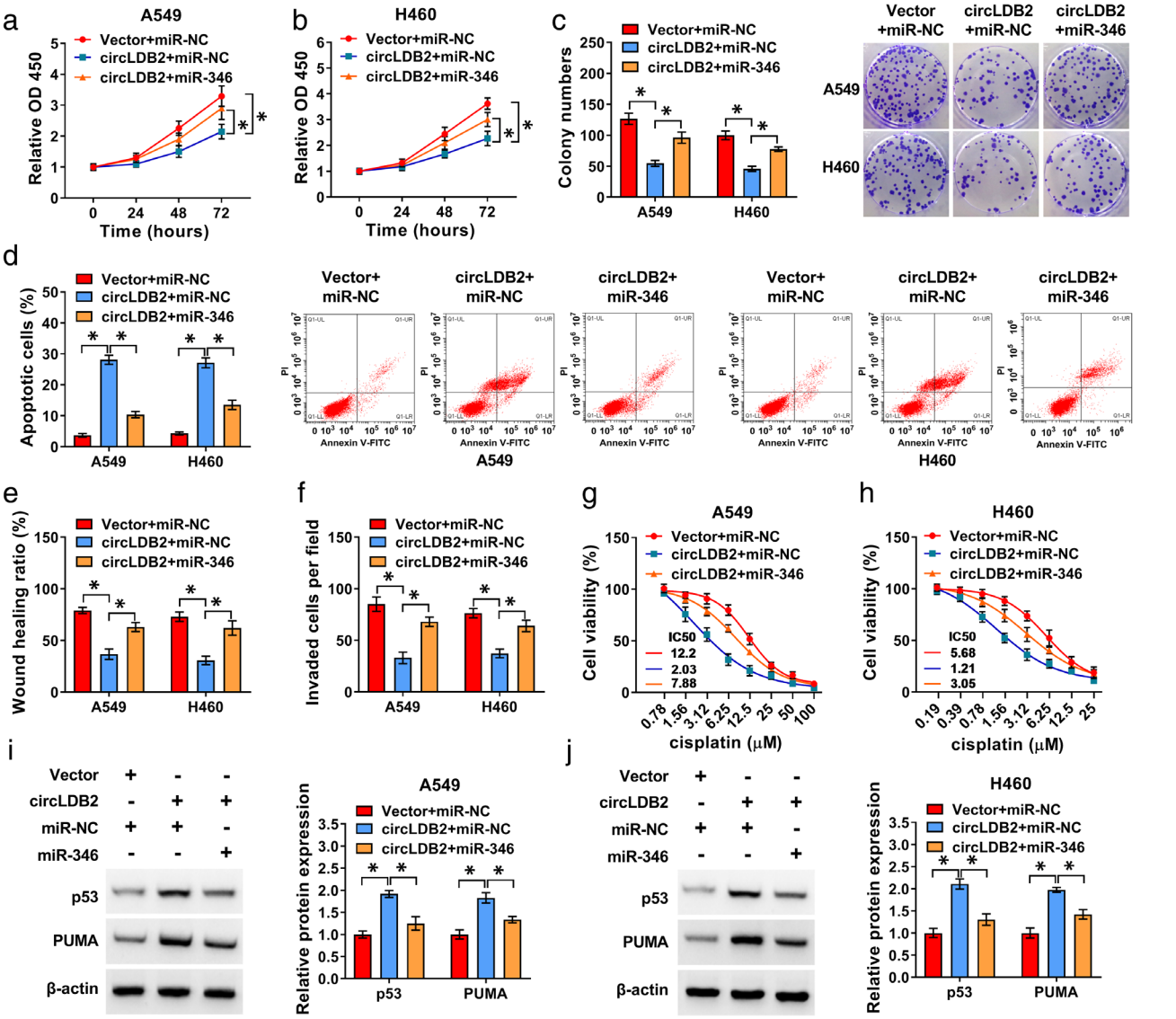

FIGURE 5 CircLDB2 regulated non-squamous NSCLC development and cisplatin sensitivity in vitro by miR-346. Vector-transduced or circLDB2-infected A549 and H460 cells were transfected with miR-NC mimic or miR-346 mimic. (a) and (b) CCK-8 assay of cell proliferation. (c) Representative images depicting a colony formation assay. (d) Representative images showing a cell apoptosis assay and flow cytometry for cell apoptosis. (e) Wound-healing assay of cell migration. (f) Cell invasion by transwell assay. (g) and (h) transfected cells were exposed to various concentrations of cisplatin, followed by the evaluation of cell viability by CCK-8 assay. (i) and (j) Western blot showing the levels of p53 and PUMA in transfected cells. $^*p < 0.05$

of anti-miR-346 was gauged by qRT-PCR (Figure 6(j),(k)). Because wound was expected, endogenous LIMCH1 protein level was reduced by miR-346 overexpression and promoted as a result of miR-346 silencing (Figure 6(l),(m)). These results together indicated that LIMCH1 was a direct target of miR-346.

Having demonstrated the function of circLDB2 as a sponge of miR-346, we wanted to explore whether circLDB2 could modulate LIMCH1 expression by acting as a ceRNA. As expected, we observed a clear increase in the level of endogenous LIMCH1 protein in circLDB2-overexpressing cells, and this effect was significantly abolished by miR-346 upregulation (Figure 6(n),(o)). Taken together, these results strongly pointed to the role of circLDB2 as a post-transcriptional regulator of LIMCH1 by sequestering miR-346.

LIMCH1 was a functionally important target of miR-346 in modulating cell functional behaviors and cisplatin sensitivity in vitro

We further asked whether LIMCH1 represented a functionally downstream target of miR-346 in modulating non-squamous NSCLC development and chemosensitivity. A vector harboring shRNA-LIMCH1 (sh-LIMCH1) was used

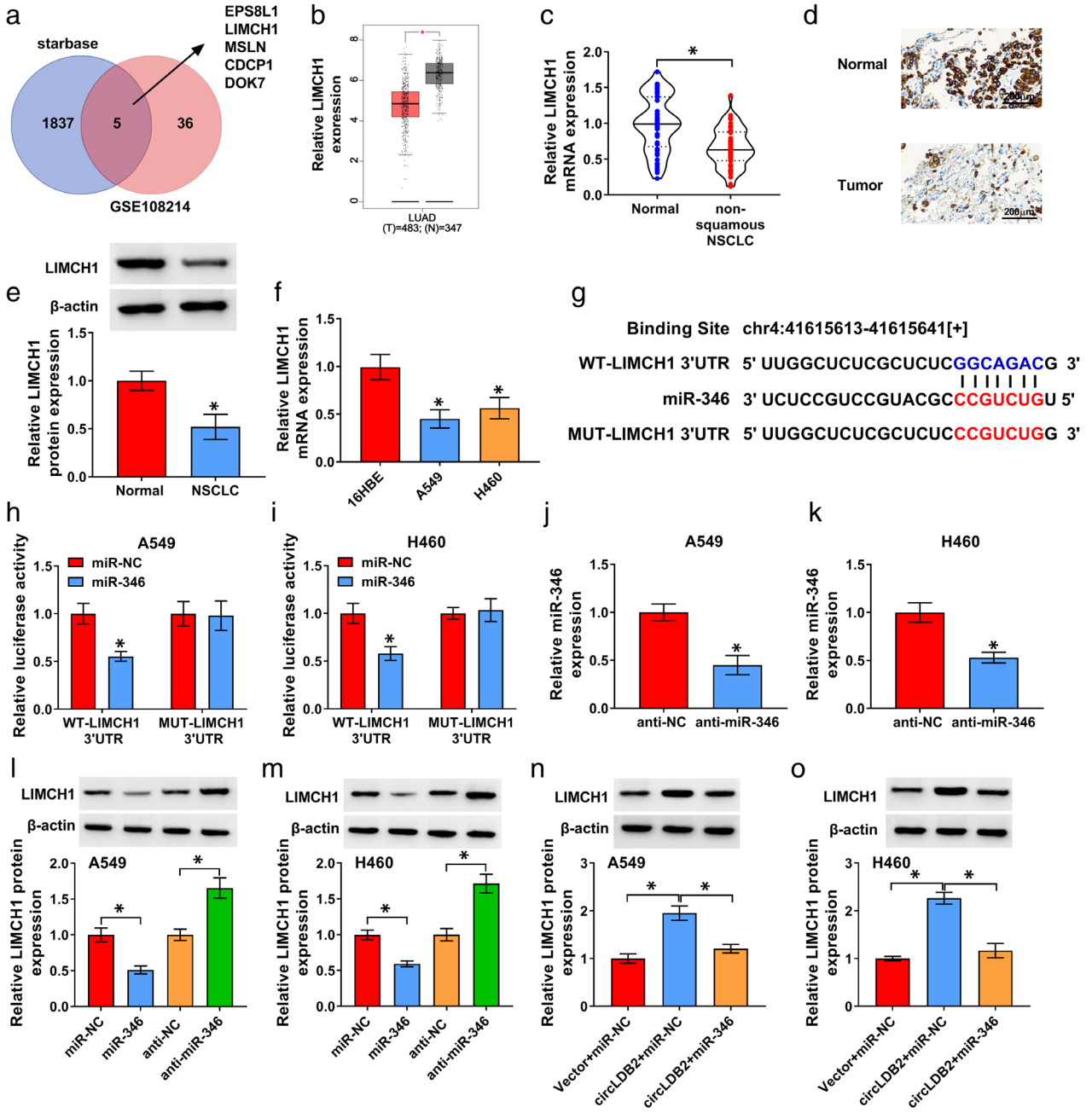

FIGURE 6 CircLDB2 modulated LIMCH1 expression by acting as a ceRNA for miR-346. (a) Venn diagram showing the putative targets of miR-346 identified by starbase software and GEO database (GSE108214). (b) the expression of LIMCH1 in LUAD and LUSC tissues compared with the controls analyzed by the GEPIA database. (c) qRT-PCR analysis of LIMCH1 mRNA in 53 primary tumors and adjacent noncancerous lung tissues from the same patients with non-squamous NSCLC. (d) Representative images depicting an immunohistochemistry assay of LIMCH1 protein expression in tissue samples. (e) Representative images depicting a western blot assay and western blot showing LIMCH1 protein in three pairs of tumor samples and adjacent noncancerous lung tissues. (f) qRT-PCR analysis showing the expression of LIMCH1 mRNA in 16HBE, A549, and H460 cells. (g) Sequence of miR-346, the miR-346 binding sites within LIMCH1 3'UTR and the mutant of the target region. (h) and (i) dual-luciferase reporter assays in A549 and H460 cells with LIMCH1 3'UTR wild-type (WT-LIMCH1 3'UTR) or mutant (MUT-LIMCH1 3'UTR) luciferase reporter constructs. (j) and (k) qRT-PCR analysis of miR-346 expression in anti-NC- or anti-miR-346-transfected A549 and H460 cells. (l) and (m) Western blot showing the expression of LIMCH1 protein in cells transfected with miR-NC mimic, miR-346 mimic, anti-NC, or anti-miR-346. (n) and (o) LIMCH1 protein level by western blot in vector-transduced or circLDB2-transduced cells transfected with miR-NC mimic or miR-346 mimic. *$p < 0.05$

to reduce the expression of LIMCH1 protein in A549 and H460 cells (Figure 7(a),(b)). Notably, reduced expression of miR-346 by anti-miR-346 transfection inhibited cell proliferation (Figure 7(c),(d)), colony formation (Figure 7(e)), and promoted cell apoptosis (Figure 7(f)), as well as impeded cell migration (Figure 7(g)) and invasion (Figure 7(h)). Moreover, miR-346 downregulation decreased the IC50 for cisplatin (Figure 7(i) and (j)) and elevated the levels of p53 and PUMA

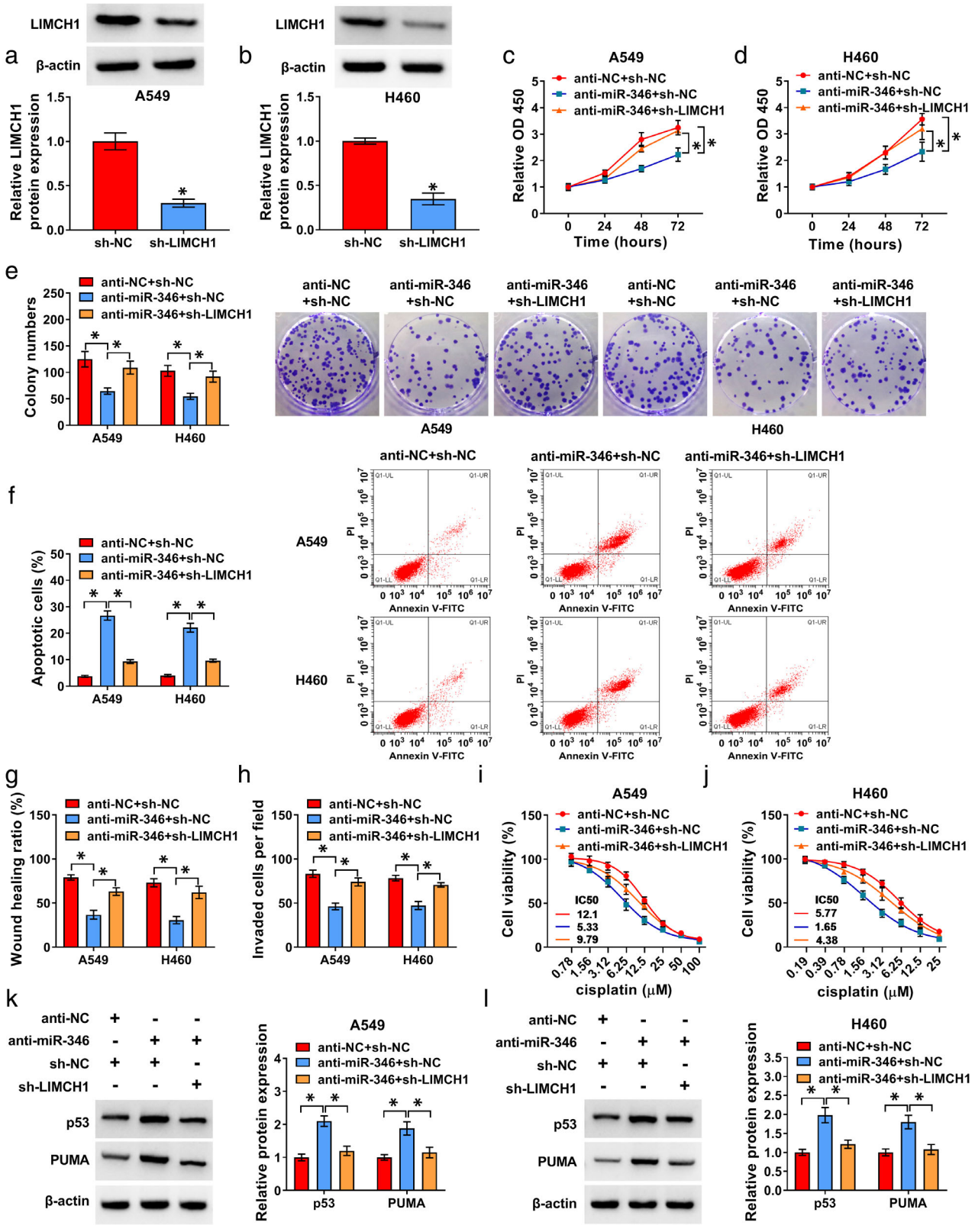

FIGURE 7 LIMCH1 was a functional target of miR-346. (a) and (b) Western blot analysis of LIMCH1 protein level in cells transfected with sh-NC or sh-LIMCH1. A549 and H460 cells were transfected with anti-NC + sh-NC, anti-miR-346 + sh-NC or anti-miR-346 + sh-LIMCH1. (c) and (d) CCK-8 assay of proliferation of transfected cells. (e) Representative images depicting a colony formation assay. (f) Representative images depicting a cell apoptosis assay and cell apoptosis by flow cytometry. (g) Wound-healing assay of cell migration. (h) Transwell assay of cell invasion. (i) and (j) CCK-8 assay for viability of transfected cells under cisplatin exposure. (k) and (l) Western blot showing the levels of p53 and PUMA in transfected cells. *$p < 0.05$

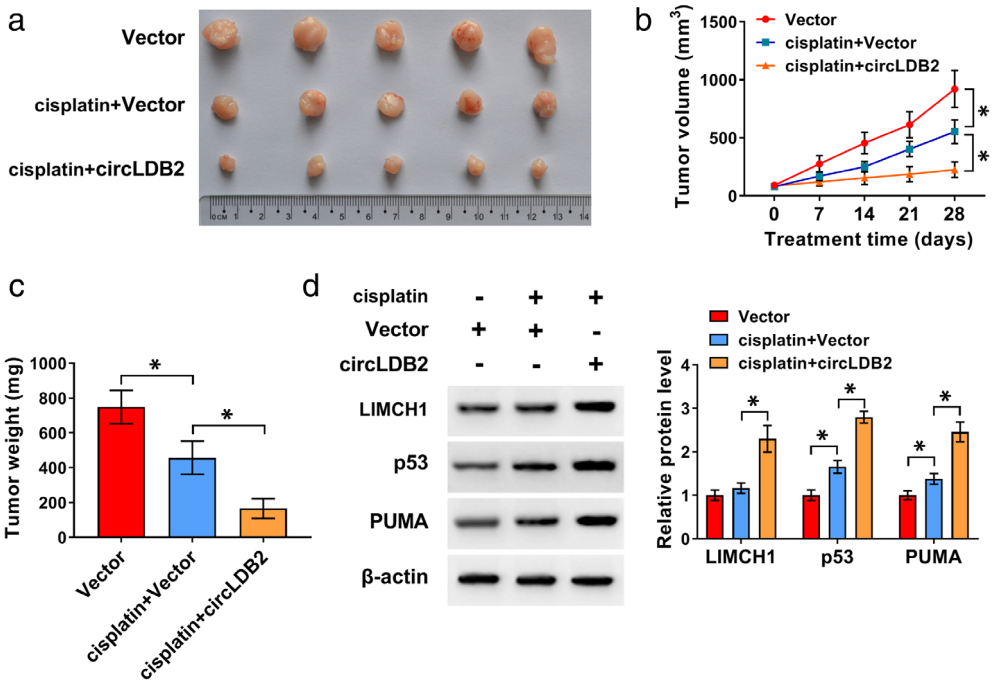

FIGURE 8 Overexpression of circLDB2 promoted the antitumor effect of cisplatin in vivo. The xenograft tumors were generated by subcutaneous injection of vector-transduced or circLDB2-transduced A549 cells (2×10^6 per mouse, n = 5 per group), and cisplatin treatment was performed twice a week by intraperitoneal injection. Mice were terminated at day 28 after cell implantation. (a) Representative images of the xenograft tumors. (b) Growth curves of the excised tumors. (c) Tumor average weight of the xenograft tumors. (d) Western blot showing the levels of LIMCH1, p53, and PUMA in the excised tumors. $^*p < 0.05$

(Figure 7(k),(l)) in both cell lines. More importantly, the cotransfection of sh-LIMCH1 remarkably abrogated these effects of miR-346 downregulation (Figure 7(c)–(l)). These results together suggested that LIMCH1 was a functional target of miR-346.

Overexpression of circLDB2 promoted the antitumor effect of cisplatin in vivo

To determine whether circLDB2 could influence the antitumor effect of cisplatin in vivo, we implanted A549 cells stably expressing circLDB2 or a scrambled control sequence (vector) into the nude mice by subcutaneous injection and administered the mice with cisplatin. As shown in Figure 8 (a)–(c), cisplatin treatment produced significantly smaller tumors than untreated controls, and circLDB2-overexpressing A549 cells produced remarkably smaller tumors than the same cells transduced with negative control under cisplatin treatment. The data of western blot showed that cisplatin treatment promoted the levels of LIMCH1, p53, and PUMA proteins in vector-transduced xenograft tumors, and simultaneous circLDB2 overexpression and cisplatin treatment led to a more significant increase in the levels of LIMCH1, p53, and PUMA proteins in the xenograft tumors (Figure 8(d)). All these results indicated that circLDB2 overexpression enhanced the antitumor effect of cisplatin in vivo.

DISCUSSION

The ceRNA hypothesis proposes that circRNAs might be crucial post-transcriptional modulators of gene expression via competing for binding to shared miRNAs.[9] Numerous studies have recently documented the implications of functional ceRNA regulation in cancer.[23] Here, we report for the first time the functional effect of circLDB2 as a new modulator of non-squamous NSCLC development and cisplatin sensitivity. Our findings identify a novel circLDB2-mediated ceRNA network in non-squamous NSCLC.

MiR-346 has been established as a potent oncomir in renal cell carcinoma, cervical cancer, and nasopharyngeal carcinoma.[24–26] Moreover, miR-346 was shown to promote breast cancer cell resistance to docetaxel.[27] Conversely, miR-346 was uncovered to impede the progression of glioma and colorectal cancer.[28,29] These contradictory findings might be, in part, because of the different types of tumors in these reports. Our results first tied in the regulation of circLDB2 in non-squamous NSCLC development and cisplatin sensitivity via sponging miR-346, which was identified as an oncomir in NSCLC.[16]

LIMCH1, a protein responsible for actin cytoskeleton remodeling, has been identified as a suppressor of cell migration via the regulation of nonmuscle myosin II.[30] Underexpression of LIMCH1 was discovered to be a potential biomarker of the prognosis of LUAD patients.[18,31] Moreover, recent work demonstrated the suppressive effect of LIMCH1 on lung cancer.[17] Our findings first showed that LIMCH1 was a direct and functional target of miR-346. We pointed to the ceRNA role of circLDB2 for miR-346 to induce LIMCH1 expression. Consistent with the previous report that LIMCH1 impeded the development of lung cancer by upregulating tumor suppressor p53 and pro-apoptotic protein PUMA,[17] we uncovered the regulation of the circLDB2/miR-346/LIMCH1 ceRNA network on p53 and PUMA expression. These findings suggested that circLDB2

controlled non-squamous NSCLC cell proliferation and apoptosis partially through the miR-346/LIMCH1/p53/PUMA network.

Cisplatin-based chemotherapy is considered the standard treatment for patients with non-squamous NSCLC.[3,4] However, chemotherapy resistance has become a major obstacle for successful treatment of patients with non-squamous NSCLC.[5,32] In vivo assays showed that circLDB2 overexpression could promote the antitumor effect of cisplatin. With these results, we envision that circLDB2 is a starting point for the improvement of chemotherapy for non-squamous NSCLC. The investigation of the precise actions of the novel ceRNA network in vivo using animal models is lacking at present, which will be performed in further work.

In summary, the current demonstration of previously uncharacterized biological actions of circLDB2, with the ability to modulate non-squamous NSCLC development and cisplatin sensitivity, pointed to its ceRNA function in non-squamous NSCLC.

CONFLICT OF INTEREST

The authors declare no conflicts of interest.

ORCID

Guojun Zhang https://orcid.org/0000-0001-8650-0847

REFERENCES

1. Bray F, Ferlay J, Soerjomataram I, Siegel RL, Torre LA, Jemal A. Global cancer statistics 2018: GLOBOCAN estimates of incidence and mortality worldwide for 36 cancers in 185 countries. CA Cancer J Clin. 2018;68:394–424.
2. Simeone JC, Nordstrom BL, Patel K, Klein AB. Treatment patterns and overall survival in metastatic non-small-cell lung cancer in a real-world, US setting. Future Oncol (London, England). 2019;15:3491–502.
3. Miyanaga A, Kubota K, Hosomi Y, Okuma Y, Minato K, Fujimoto S, et al. Phase II trial of S-1 plus cisplatin combined with bevacizumab for advanced non-squamous non-small cell lung cancer (TCOG LC-1202). Jpn J Clin Oncol. 2019;49:749–54.
4. Paz-Ares L, Mezger J, Ciuleanu TE, Fischer JR, von Pawel J, Provencio M, et al. Necitumumab plus pemetrexed and cisplatin as first-line therapy in patients with stage IV non-squamous non-small-cell lung cancer (INSPIRE): an open-label, randomised, controlled phase 3 study. Lancet Oncol. 2015;16:328–37.
5. Gao Y, Dorn P, Liu S, Deng H, Hall SRR, Peng RW, et al. Cisplatin-resistant A549 non-small cell lung cancer cells can be identified by increased mitochondrial mass and are sensitive to pemetrexed treatment. Cancer Cell Int. 2019;19:317.
6. Van Der Steen N, Lyu Y, Hitzler AK, Becker AC, Seiler J, Diederichs S. The circular RNA landscape of non-small cell lung cancer cells. Cancer. 2020;12:1091.
7. Park SJ, More S, Murtuza A, Woodward BD, Husain H. New targets in non-small cell lung cancer. Hematol Oncol Clin North Am. 2017;31:113–29.
8. Memczak S, Jens M, Elefsinioti A, Torti F, Krueger J, Rybak A, et al. Circular RNAs are a large class of animal RNAs with regulatory potency. Nature. 2013;495:333–8.
9. Tay Y, Rinn J, Pandolfi PP. The multilayered complexity of ceRNA crosstalk and competition. Nature. 2014;505:344–52.
10. Song L, Cui Z, Guo X. Comprehensive analysis of circular RNA expression profiles in cisplatin-resistant non-small cell lung cancer cell lines. Acta Biochim Biophys Sin (Shanghai). 2020;52:944–53.
11. Chi Y, Luo Q, Song Y, Yang F, Wang Y, Jin M, et al. Circular RNA circPIP5K1A promotes non-small cell lung cancer proliferation and metastasis through miR-600/HIF-1α regulation. J Cell Biochem. 2019;120:19019–30.
12. Chen L, Nan A, Zhang N, Jia Y, Li X, Ling Y, et al. Circular RNA 100146 functions as an oncogene through direct binding to miR-361-3p and miR-615-5p in non-small cell lung cancer. Mol Cancer. 2019;18:13.
13. Xu X, Tao R, Sun L, Ji X. Exosome-transferred hsa_circ_0014235 promotes DDP chemoresistance and deteriorates the development of non-small cell lung cancer by mediating the miR-520a-5p/CDK4 pathway. Cancer Cell Int. 2020;20:552.
14. Florczuk M, Szpechcinski A, Chorostowska-Wynimko J. miRNAs as biomarkers and therapeutic targets in non-small cell lung cancer: current perspectives. Target Oncol. 2017;12:179–200.
15. Arab A, Karimipoor M, Irani S, Kiani A, Zeinali S, Tafsiri E, et al. Potential circulating miRNA signature for early detection of NSCLC. Cancer Genet. 2017;216–217:150–8.
16. Sun CC, Li SJ, Yuan ZP, Li DJ. MicroRNA-346 facilitates cell growth and metastasis, and suppresses cell apoptosis in human non-small cell lung cancer by regulation of XPC/ERK/snail/E-cadherin pathway. Aging (Albany NY). 2016;8:2509–24.
17. Zhang Y, Zhang Y, Xu H. LIMCH1 suppress the growth of lung cancer by interacting with HUWE1 to sustain p53 stability. Gene. 2019;712:143963.
18. Karlsson T, Kvarnbrink S, Holmlund C, Botling J, Micke P, Henriksson R, et al. LMO7 and LIMCH1 interact with LRIG proteins in lung cancer, with prognostic implications for early-stage disease. Lung Cancer. 2018;125:174–84.
19. Korpal M, Ell BJ, Buffa FM, Ibrahim T, Blanco MA, Celià-Terrassa T, et al. Direct targeting of Sec23a by miR-200s influences cancer cell secretome and promotes metastatic colonization. Nat Med. 2011;17:1101–8.
20. Xu M, Chen X, Lin K, Zeng K, Liu X, Pan B, et al. The long noncoding RNA SNHG1 regulates colorectal cancer cell growth through interactions with EZH2 and miR-154-5p. Mol Cancer. 2018;17:141.
21. Pijuan J, Barceló C, Moreno DF, Maiques O, Sisó P, Marti RM, et al. In vitro cell migration, invasion, and adhesion assays: from cell imaging to data analysis. Front Cell Dev Biol. 2019;7:107.
22. Iwakawa HO, Tomari Y. The functions of MicroRNAs: mRNA decay and translational repression. Trends Cell Biol. 2015;25:651–65.
23. Karreth FA, Pandolfi PP. ceRNA cross-talk in cancer: when ce-bling rivalries go awry. Cancer Discov. 2013;3:1113–21.
24. Su ZH, Liao HH, Lu KE, Chi Z, Qiu ZQ, Jiang JM, et al. Hypoxia-responsive miR-346 promotes proliferation, migration, and invasion of renal cell carcinoma cells via targeting NDRG2. Neoplasma. 2020;67:1002–11.
25. Guo J, Lv J, Liu M, Tang H. miR-346 up-regulates Argonaute 2 (AGO2) protein expression to augment the activity of other MicroRNAs (miRNAs) and contributes to cervical cancer cell malignancy. J Biol Chem. 2015;290:30342–50.
26. Yan HL, Li L, Li SJ, Zhang HS, Xu W. miR-346 promotes migration and invasion of nasopharyngeal carcinoma cells via targeting BRMS1. J Biochem Mol Toxicol. 2016;30:602–7.
27. Yang F, Luo LJ, Zhang L, Wang DD, Yang SJ, Ding L, et al. MiR-346 promotes the biological function of breast cancer cells by targeting SRCIN1 and reduces chemosensitivity to docetaxel. Gene. 2017;600:21–8.
28. Li Y, Xu J, Zhang J, Zhang J, Zhang J, Lu X. MicroRNA-346 inhibits the growth of glioma by directly targeting NFIB. Cancer Cell Int. 2019;19:294.
29. Liang Y, Shi J, He Q, Sun G, Gao L, Ye J, et al. Hsa_circ_0026416 promotes proliferation and migration in colorectal cancer via miR-346/NFIB axis. Cancer Cell Int. 2020;20:494.
30. Lin YH, Zhen YY, Chien KY, Lee IC, Lin WC, Chen MY, et al. LIMCH1 regulates nonmuscle myosin-II activity and suppresses cell migration. Mol Biol Cell. 2017;28:1054–65.
31. Cao H, Zhao J, Chen Z, Sun W, Ruan K, Zhou J, et al. Loss of LIMCH1 predicts poor prognosis in patients with surgically resected

lung adenocarcinoma: a study based on Immunohistochemical analysis and bioinformatics. J Cancer. 2021;12:181–9.
32. Sarin N, Engel F, Kalayda GV, Mannewitz M, Cinatl J, Rothweiler F, et al. Cisplatin resistance in non-small cell lung cancer cells is associated with an abrogation of cisplatin-induced G2/M cell cycle arrest. PloS One. 2017;12:e0181081.

SUPPORTING INFORMATION

Additional supporting information may be found online in the Supporting Information section at the end of this article.

How to cite this article: Wang Y, Li L, Zhang W, Zhang G. Circular RNA circLDB2 functions as a competing endogenous RNA to suppress development and promote cisplatin sensitivity in non-squamous non-small cell lung cancer. Thorac Cancer. 2021;12:1959–1972. https://doi.org/10.1111/1759-7714.13993